Optical Voltage Sensors

Deutsche Ausgabe: DOI: 10.1002/ange.201508586
Internationale Ausgabe: DOI: 10.1002/anie.201508586

# Plasmonic/Nonlinear Optical Material Core/Shell Nanorods as Nanoscale Plasmon Modulators and Optical Voltage Sensors

*Anxiang Yin, Qiyuan He, Zhaoyang Lin, Liang Luo, Yuan Liu, Sen Yang, Hao Wu, Mengning Ding, Yu Huang, and Xiangfeng Duan**

***Abstract:*** *Herein, we report the design and synthesis of plasmonic/non-linear optical (NLO) material core/shell nanostructures that can allow dynamic manipulation of light signals using an external electrical field and enable a new generation of nanoscale optical voltage sensors. We show that gold nanorods (Au NRs) can be synthesized with tunable plasmonic properties and function as the nucleation seeds for continued growth of a shell of NLO materials (such as polyaniline, PANI) with variable thickness. The formation of a PANI nanoshell allows dynamic modulation of the dielectric environment of the plasmonic Au NRs, and therefore the plasmonic resonance characteristics, by an external electrical field. The finite element simulation confirms that such modulation is originated from the field-induced modulation of the dielectric constant of the NLO shell. This approach is general, and the coating of the Au NRs with other NLO materials (such as barium titanate, BTO) is found to produce a similar effect. These findings can not only open a new pathway to active modulation of plasmonic resonance at the sub-wavelength scale but also enable the creation of a new generation of nanoscale optical voltage sensors (NOVS).*

The local surface plasmonic resonance (LSPR) property of noble metal (for example, Au and Ag) nanostructures can allow for light manipulation at the sub-wavelength scale,[1,2] and enable exciting technological opportunities in diverse fields, including sensing,[3–5] photovoltaics,[6,7] catalysis,[8,9] and optical antennas.[10,11] The plasmonic resonance properties of noble metal nanostructures can be controlled by the composition, size, morphology, and the surrounding dielectric environment.[12–14] The composition, size, and morphology of a given plasmonic nanostructure are fixed and cannot be varied in a dynamic way after the initial synthesis or fabrication. Thus, the manipulation of the surrounding dielectric environment becomes the only way to modulate the plasmonic resonance for diverse applications.[15–24] Considerable efforts have been devoted to investigating the interaction between plasmonic nanostructures and the surrounding environments, such as electro- and photo-chromic molecules,[15,16] inorganic materials,[17,18] polymers,[19–21] and liquid crystals.[22–24] On one hand, the plasmonic resonance can substantially modify the optical properties of the nearby materials, for example, to enhance the absorption or accelerate the radiative decay rate.[25–27] On the other hand, the variation of the surrounding dielectric environment may significantly alter the plasmonic resonance properties of the metallic nanostructures.[12–14] Therefore, the integration of plasmonic nanostructures with active dielectric materials can enable the active modulation of the plasmonic resonance by using an external trigger (for example, light, heat, electric potential) and may open up a pathway to advanced nanodevices, including active metamaterials,[28] smart windows,[29] and displays,[30] as well as a new generation of nanoscale sensors that can sensitively monitor local environmental changes.

Herein, we explore the interaction between plasmonic nanostructures and NLO materials to enable active modulation of the dielectric environment and thus plasmonic properties by an external electrical field. We chose Au nanorods (NRs) with specific aspect ratio as a model system owing to their high stability, strong and tunable plasmonic resonance in the visible region, and high sensitivity to changes in the surrounding dielectric environment.[31] We examined both the organic polyaniline (PANI) and inorganic barium titanium oxide (BTO) as two examples of typical NLO materials. PANI represents a typical semiconducting polymer with tunable conductivity, dielectric function, and thus excellent NLO properties.[32–34] BTO is a typical perovskite-type inorganic material with unique ferroelectric and electro-optic properties, which is more applicable for ultrafast optical switches, but usually with smaller piezoelectric coefficients as compared to organic NLO materials. The Au NRs and NLO materials were integrated together to form Au/NLO core/shell NRs (Figure 1a), and modulation of the plasmonic properties by an external electrical field was studied by using a single particle scattering spectroscopy approach (Figure 1b). The Au/PANI NRs exhibit a significant, robust, and reversible plasmon peak shift when triggered by an external electric field. The electrically switching behavior for these plasmonic NRs shows a strong dependence on the NR orientation, the electric field direction, and the polarization direction of the incident light. Furthermore, we also demonstrate that this concept can be extended to Au/BTO core/shell NRs and show similar electro-optical modulation.

[*] Dr. A. Yin, Dr. Q. He, Z. Lin, Dr. L. Luo, Prof. X. Duan
Department of Chemistry and Biochemistry
University of California
Los Angeles, CA 90095 (USA)
E-mail: xduan@chem.ucla.edu
Y. Liu, S. Yang, H. Wu, Dr. M. Ding, Prof. Y. Huang
Department of Materials Science and Engineering
University of California
Los Angeles, CA 90095 (USA)
Prof. Y. Huang, Prof. X. Duan
California Nanosystems Institute, University of California
Los Angeles, CA 90095 (USA)

Supporting information for this article is available on the WWW under http://dx.doi.org/10.1002/anie.201508586.

  

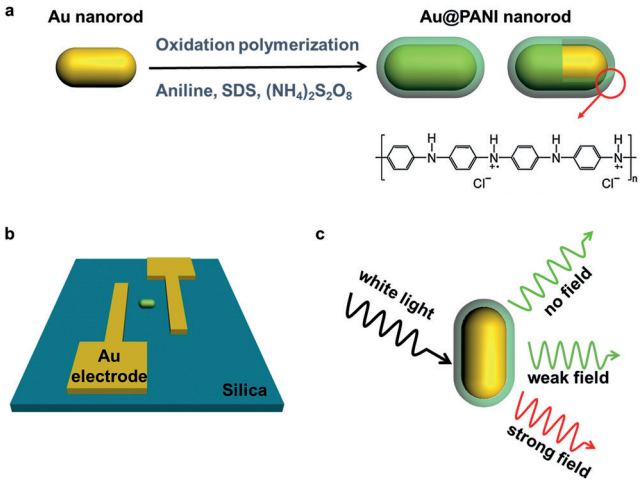


***Figure 1.*** Design of Au/PANI NRs as a single-particle plasmonic resonance modulator and nanoscale optical voltage sensor (NOVS). a) The design and synthesis of Au/PANI NRs. b) Illustration of field-dependent single particle spectroscopy. c) Voltage-modulated LSPR scattering, illustrating a local electric-field-induced shift of the scattering peak.

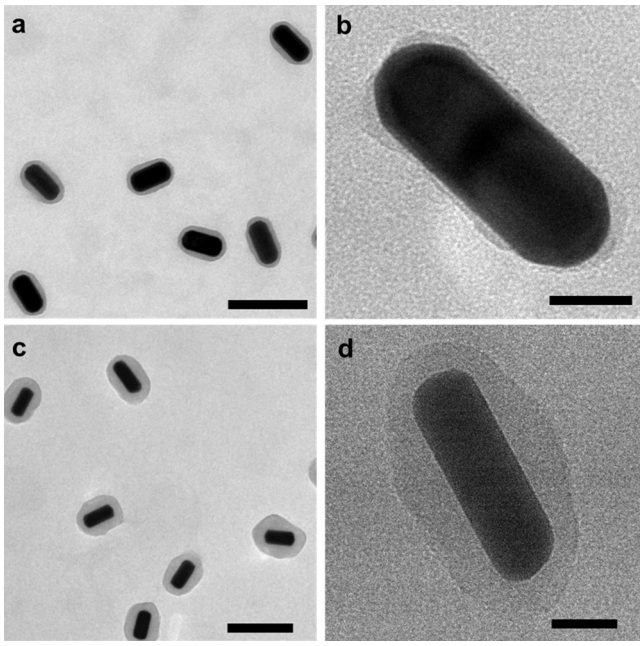


***Figure 2.*** TEM images for Au/PANI NRs with different shell thicknesses. a, b) TEM images for Au/PANI NRs with a shell thickness of about 5 to 10 nm. c, d) TEM images for Au//PANI NRs with a shell thickness of about 20 nm. Scale bar: 200 nm (a, c), 20 nm (b, d).

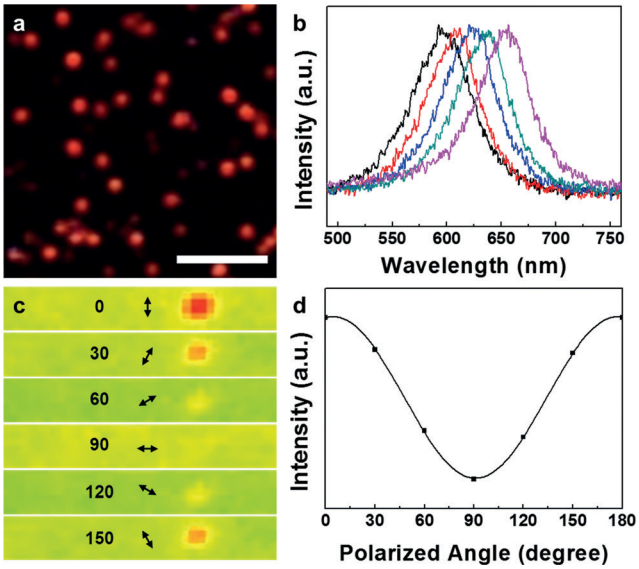


***Figure 3.*** Single particle scattering image and spectroscopy for Au/PANI NRs. a) Dark-field image of individual Au/PANI NRs on quartz substrates. Scale bar: 10 μm. b) Single particle scattering spectra for Au/PANI NRs with different aspect ratios. c) False-color scattering images for a single Au/PANI NR under the incident light of variable polarization directions. d) The polarization dependence of the scattering intensity for the Au/PANI NR shown in panel c.

Au NRs with controlled aspect ratios and tunable LSPR scattering frequencies were prepared using a seeded method with cetyltrimethylammonium bromide (CTAB) as the stabilizing and structure directing agent.[35,36] We have chosen Au NRs with a proper aspect ratio as our model system to ensure the scattering spectra were located in the visible range for the convenience of our study (Supporting Information, Figure S1). A similar strategy can be applied to other plasmonic nanostructures with different plasmon resonance frequencies. A uniform PANI shell was coated onto the Au NRs with controllable thickness using a modified oxidative polymerization method.[37] In brief, a mixture solution of sodium dodecylsulfate (SDS) and aniline was added into the CTAB-capped Au NR solution. A strong oxidant, $(NH_4)_2S_2O_8$, was then introduced into the mixture and the polymerization of aniline occurred on the surface of the Au NRs, producing a PANI shell on the surface of Au NRs. The resulting Au/PANI NRs were separated from the solution through a centrifugation process. The thickness of the PANI coating can be controlled in the range of 5–20 nm by tuning the molar ratio of aniline monomers, or by repeating the coating process multiple times (Figure 2).

To inspect the plasmonic properties of individual nanoparticles, the Au/PANI NRs were deposited onto silicon/silicon oxide or quartz substrates using a dip-coating method. The scattering images or spectra for individual Au/PANI core/shell NRs were collected using a dark-field optical microscope (with a 50 × Olympus dark-field objective, NA = 0.50) with an integrated monochromator (Acton SpectraPro 2300i), and a liquid-nitrogen-cooled CCD camera (Princeton Instruments Spec10; Figure S2). The individual NRs can be readily identified under the dark-field optical microscope (Figure 3a), and the corresponding scattering spectra for a single Au/PANI NR can be collected by the integrated spectrometer (Figure 3b). The single-particle spectroscopy of the Au/PANI NR reveals a plasmonic resonance peak between 590 and 660 nm, corresponding to the longitudinal plasmon resonance mode of the NRs, which may be readily tuned by varying the aspect ratios of the Au NRs (Figure S1). For convenience and spectral matching with sensitivity of our CCD cameras, we have focused on NRs with LSPR peaks

around 620 nm to probe the electrical-field-modulated plasmonic properties. It is important to note that the longitudinal LSPR scattering spectra for a single Au/PANI NR is strongly dependent on the polarization direction of the incident light (Figure 3c,d). The scattering intensity can reach its maximum value when the polarization direction is parallel to the longitudinal NR axis. When the polarization direction is perpendicular to the longitudinal NR axis, no obvious scattering image or spectral peak can be observed because the transverse LSPR is too weak. In this way, the long axis of a specific NR can be determined by rotating a polarizer between the incident light and the specimen. The orientation of the NR longitudinal axis corresponds to the polarization direction at which the LSPR scattering intensity reaches the maximum value.

To probe the electrical-field-modulated plasmonic resonance properties of individual nanoparticles, the Au/PANI NRs were deposited onto a quartz substrate between a pair of lithographically patterned electrodes, through which a modulating electrical field can be applied (Figure 4a; Supporting Information, Figure S3). The electrical field modulation of the plasmonic resonance is strongly dependent on the NR axis direction and the field direction. We have therefore employed polarized incident light to identify the NR orientation and probe the effect of the relative orientation between the NR axis and the electric field direction. For all of the single particle spectroscopic studies, we have employed an incident light with the polarization parallel to the NR axis to maximize the plasmonic resonance signal. We have first focused on NRs with the longitudinal axis parallel to the electrical field direction to study the effect of electric fields on their LSPR characteristics. Importantly, when the polarization of the incident light and the NR axis is in parallel to the electrical field direction, an obvious field-induced modulation of the plasmonic peak can be observed (Figure 4b). The scattering spectrum for a single Au/PANI NR shows a peak at 613.3 nm without a local electric field (the "off" state), which redshifts to 624.0 nm when an external electric field of $\approx 10\ V\,\mu m^{-1}$ was applied. As a comparison, no apparent shift can be observed when the bare Au NRs are used in the experiment (Figure S4). This obvious redshift of the LSPR spectra under an external electrical field can be ascribed to the active modulation of the dielectric environment, and therefore the plasmonic resonance characteristics (see below). On the other hand, when the long axis of NR is perpendicular to the field direction, no obvious field-induced modulation can be observed (Figure 4c). Furthermore, when the polarization direction of the incident light is normal to the NR long axis, no contributions from the longitudinal LSPR can be collected, and the transverse LSPR scattering is too weak to be observed at the single particle level. Thus, no significant external field effect can be seen regardless of the relative orientation of the electric field versus the NR axis (Figure S5).

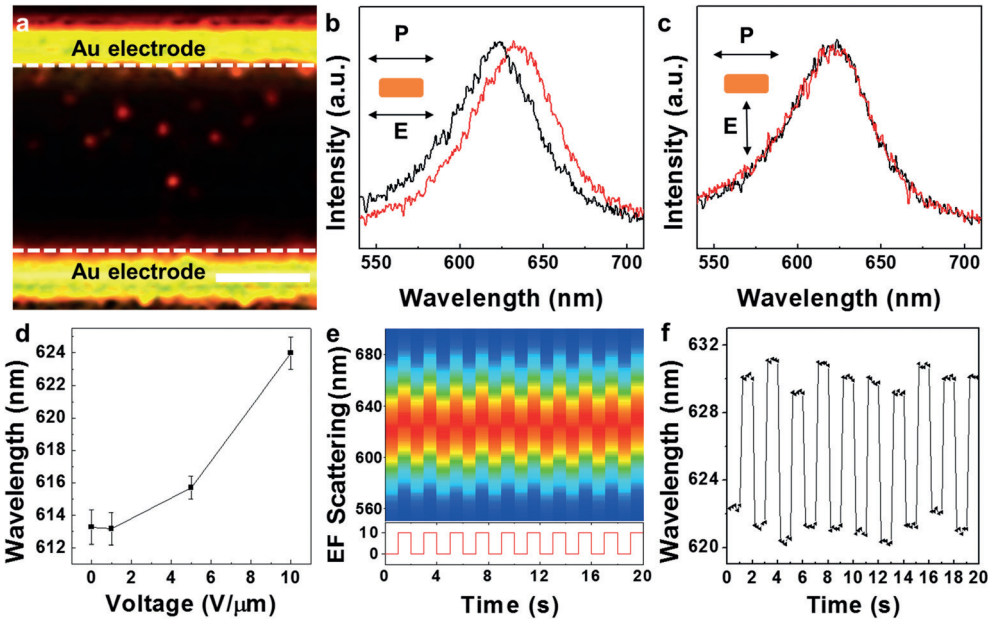


***Figure 4.*** Dynamic modulation of LSPR scattering spectra of a single Au/PANI NR by an external electric field. a) Dark-field image for Au/PANI NRs between a pair of electrodes on quartz substrates. Scale bar: 5 μm. b) The LSPR spectra with (red) and without (black) parallel electrical fields. c) No obvious modulation of LSPR spectra is observed when the electrical field direction is perpendicular to the NR axis. The electric field ($10\ V\,\mu m^{-1}$) is set to "off" (black) or "on" (red). The arrows labeled with P and E shown in the insets represent the directions of the polarization of the incident light and the external electric field, respectively. d) Spectral shifts of the LSPR peak for a single Au/PANI NR under different electrical fields (10 measurements for each point). e) A series of 100 successive spectra obtained from a single Au/PANI NR under a periodically modulating field. The field modulation frequency is 1 Hz, and the single frame integration for each spectra is 200 ms (5 frames of spectra for each on/off window). The unit for the electric field (EF) in the lower part is $V\,\mu m^{-1}$. f) The switch of LSPR peak position with on/off electrical field ($10\ V\,\mu m^{-1}$).

We have also studied the modulation of the plasmonic response of the single Au/PANI NR by varying external fields (Figure 4d). When the external field was relatively low (for example, $1\ V\,\mu m^{-1}$), no significant redshift could be observed. With increasing electrical field to 5 and $10\ V\,\mu m^{-1}$, the redshift increases to 2.5 and 10.7 nm, respectively. The non-linear increase of the wavelength shift is due to the polarization of the PANI shell by the external electric field, which combines the non-linear Kerr effect and the linear Pockels effect.[32,33] Such electrical field modulation of plasmonic resonance is reversible and can be readily switch back and forth. Reversible switching of LSPR by the external electric field was revealed by continuously recording the

  

LSPR spectra under a periodic modulating electrical field (10 V μm$^{-1}$; Figure 4e,f; Supporting Information, Figure S6). Figure 4e shows 100 successive spectra of a single NR under electric field modulations. The time window for each off/on period is 1 s (1 Hz), and 5 spectra were taken during each window with the integration time of 200 ms for each spectrum. A significant redshift can be observed immediately (within the time resolution of our measurement) as the electric field is turned on/off, yet no obvious difference can be seen in the 5 spectra within each window (Figure 4e,f). These studies demonstrate that the LSPR spectra of these Au/PANI NRs can show a significant, rapid, and reversible response to the varying external electric field.

To further confirm the field-dependent behavior of the Au/PANI NRs, we have employed the finite element method (using COMSOL simulation package) to simulate the modulation of LSPR characteristics of Au NRs in varying dielectric environment. An Au NR core with a 20 nm thick PANI shell is used in the simulation (Figure 5, inset). PANI

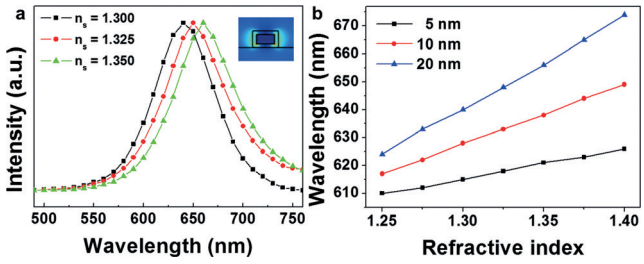


***Figure 5.*** Simulation of LSPR spectral shift for a single Au/PANI NR with different refractive index ($n_s$) of the surrounding medium and different shell thickness. a) Simulated LSPR spectra for a NR (aspect ratio of 1.6) with a shell (20 nm) of different refractive indices. b) LSPR spectral peak vs. shell refractive index for NRs with different shell thickness (5, 10, and 20 nm). The substrate is quartz (silica) and the upper atmosphere is air for all simulations.

was treated as a dielectric material with its dielectric function obtained from a recent report.[38] By adapting the varying dielectric constant into the COMSOL simulation package, our simulation shows that a change of the refractive index by 0.05 in NLO shell can induce a redshift as large as 20 nm in the scattering spectra for a single Au/PANI core/shell NR with the aspect ratio of 1.6 (Figure 5a). The redshift is also dependent on the thickness of the PANI shell (Figure 5b). For example, Au/PANI NRs with 5 nm of PANI shell show no significant redshifts in their LSPR peaks (less than 5 nm) when the refractive index of the surrounding medium increases 0.05, which was confirmed by our experimental results (Figure S7). These simulation results match well with our experimental data, and thus indicate that the Au/PANI NRs can be employed as an excellent optical voltage sensor.

The above studies clearly demonstrate that our design of plasmonic/NLO core/shell nanostructures can exhibit a unique electro-optical modulation effect. To further demonstrate the generality of this concept, we have also coated the Au NRs with other NLO materials (for example, BTO). The Au/BTO core/shell NRs with a shell thickness of ≈20 nm were prepared using a seeded hydrolysis method followed by a hydrothermal treatment. As an inorganic NLO material with local polarization structures, the dielectric constant of BTO can be modulated by an external electrical field, and the difference in the refractive index can be as large as 0.05.[39] In our experiment, when an external electric field of 20 V μm$^{-1}$ was applied, a redshift of the LSPR peak by about 9 nm was observed (from 670 to 679 nm in Figure S8). Such field-induced spectral shift may be further improved by increasing the BTO shell thickness or improving the BTO shell crystallinity.[40]

The electrical-field-induced modulation of the LSPR in Au/PANI NRs can be attributed to the synergistic effects of both the electro-optic properties of the PANI shell and the LSPR characteristics of the Au core. As a NLO polymer, PANI can be significantly polarized by an external electric field.[32,33] The electric field could change either the dipole orientations of the aniline unit in the polymer chain or the free aniline molecules entrapped in the PANI shell. The change of the dipole orientation and the increase of the dipole moment would then increase the dielectric constant of the PANI shell. Meanwhile, the plasmonic resonance of the embedded Au core is very sensitive to the change of the dielectric constant of the surrounding environments.[41,42] Together, the alteration of the dielectric constant of the outer NLO shell by an external electric field can lead to a detectable redshift in LSPR scattering spectra. When the electric field is parallel to the long axis of the Au/PANI NR, the voltage would alter the dipole orientation of the polymerized or free aniline molecules and thus cause the increase of the dielectric constant along the long axis direction, resulting in a redshift of the LSPR spectra in the plasmonic cores.

In summary, through close integration of plasmonic and NLO materials into a core/shell nanostructure, we have designed a nanoscale plasmonic modulator. We show polymer (PANI) or inorganic (BTO) shells can be coated onto Au NRs to realize these nanosized, sub-wavelength electro–optic modulators.[45] Single particle scattering spectroscopy studies show that the plasmonic resonance of the Au NRs can be reversibly switched by an external electric-field-induced modulation of the dielectric function of the NLO shell. The electrically switching behavior shows a strong dependence on the NR orientations, the electric field direction, and the polarization direction of the incident light. The LSPR/NLO NRs represent a simple optical antenna that can be modulated remotely. The described strategy can be translated to more complicated antenna architectures for optical probes monitoring variations of local electric field, or for remote electric manipulation of visible light at the sub-wavelength scale. Moreover, we anticipate these devices can be improved in terms of operating voltage by carefully selecting the plasmonic cores and other NLO materials. Our Au/NLO NRs provide a general and robust method for the design and fabrication of sub-wavelength "electric-plasmonic-optical" modulators and nanoscale optical voltage sensors (NOVS). They can broadly impact areas including nanoscale electro-optics and in vitro or in vivo voltage sensors for highly parallel monitoring of cellular membrane potentials in real-time. Our

designed structures show robust spectral shifts at room temperature, in contrast to the quantum-confined Stark effect in semiconductor nanoparticles that typically require low temperature environments,[43] or show much smaller spectral shifts under the same electrical field.[44] The chemical preparation of LSRP/NLO nanoparticles with different plasmonic cores (such as Au and Ag) and NLO shells and their applications for monitoring cell membrane potentials are currently underway in our laboratory.

## Acknowledgements

We acknowledge financial support of this work by Human Frontier Science Program Young Investigator Fellowship RGY0077.

**Keywords:** gold nanorods · nonlinear optical materials · polyanilines · surface plasmon resonance · voltage sensors

**How to cite:** *Angew. Chem. Int. Ed.* **2016**, *55*, 583–587
*Angew. Chem.* **2016**, *128*, 593–597

[1] S. Lai, S. Link, N. J. Halas, *Nat. Photonics* **2007**, *1*, 641–648.
[2] J. A. Schuller, E. S. Barnard, W. S. Cai, Y. C. Jun, J. S. White, M. L. Brongersma, *Nat. Mater.* **2010**, *9*, 193–204.
[3] N. Liu, M. L. Tang, M. Hentschel, H. Giessen, A. P. Alivisatos, *Nat. Mater.* **2011**, *10*, 631–636.
[4] C. H. Wu, A. B. Khanikaev, R. Adata, N. Arju, A. A. Yanik, H. Altug, G. Shvets, *Nat. Mater.* **2011**, *11*, 69–75.
[5] W. C. Tan, M. Hofmann, Y. P. Hsieh, M. L. Lu, Y. F. Chen, *Nano Res.* **2012**, *5*, 695–702.
[6] H. A. Atwater, A. Polman, *Nat. Mater.* **2010**, *9*, 205–213.
[7] D. H. Wang, D. Y. Kin, K. W. Choi, J. H. Seo, S. H. Im, J. H. Park, O. O. Park, A. J. Heeger, *Angew. Chem. Int. Ed.* **2011**, *50*, 5519–5523; *Angew. Chem.* **2011**, *123*, 5633–5637.
[8] S. Linic, P. Christopher, D. B. Ingram, *Nat. Mater.* **2011**, *10*, 911–921.
[9] F. Wang, C. H. Li, H. J. Chen, R. B. Jiang, L. D. Sun, Q. Li, J. F. Wang, C. H. Yan, *J. Am. Chem. Soc.* **2013**, *135*, 5588–5601.
[10] T. Kosako, Y. Kodoya, H. F. Hofmann, *Nat. Photonics* **2010**, *4*, 312–315.
[11] A. G. Curto, G. Volpe, T. H. Taminiau, M. P. Kreuzer, R. Quidant, N. F. van Hulst, *Science* **2010**, *329*, 930–933.
[12] S. E. Skrabalak, J. Y. Chen, Y. G. Sun, X. M. Lu, L. Au, C. M. Cobley, Y. N. Xia, *Acc. Chem. Res.* **2008**, *41*, 1587.
[13] H. J. Chen, L. Shao, Q. Li, J. F. Wang, *Chem. Soc. Rev.* **2013**, *42*, 2679–2724.
[14] Y. H. Sun, L. Jiang, L. B. Zhong, Y. Y. Jiang, X. D. Chen, *Nano Res.* **2015**, *8*, 406–417.
[15] T. Ming, L. Zhao, M. D. Xiao, J. F. Wang, *Small* **2010**, *6*, 2514–2519.
[16] Y. B. Zheng, B. Kiraly, S. Cheunkar, T. J. Huang, P. S. Weiss, *Nano Lett.* **2011**, *11*, 2061–2065.
[17] J. Y. Suh, E. U. Donev, R. Lopez, L. C. Feldman, R. F. Haglund, Jr., *Appl. Phys. Lett.* **2006**, *88*, 133115.
[18] W. L. Gao, G. Shi, Z. H. Jin, J. Shu, Q. Zhang, R. Vajtai, P. M. Ajayan, J. Kono, Q. F. Xu, *Nano Lett.* **2013**, *13*, 3698–3702.
[19] Y. R. Leroux, J. C. Lacroix, K. I. Chane-Ching, C. Fave, N. Felidj, G. Levi, J. Aubard, J. R. Krenn, A. Hohenau, *J. Am. Chem. Soc.* **2005**, *127*, 16022–16023.
[20] Y. Leroux, J. C. Larroix, C. Fave, G. Trippe, N. Felidj, J. Aubard, A. Hohenau, J. R. Krenn, *ACS Nano* **2008**, *2*, 728–732.
[21] V. Stockhausen, P. Martin, J. Ghilane, Y. Leroux, H. Randriamahazaka, J. Grand, N. Felidj, J. C. Lacroix, *J. Am. Chem. Soc.* **2010**, *132*, 10224–10226.
[22] P. A. Kossyrev, A. J. Yin, S. G. Cloutier, D. A. Cardimona, D. P. Huang, P. M. Alsing, J. M. Xu, *Nano Lett.* **2005**, *5*, 1978–1981.
[23] W. Dickson, G. A. Wurtz, P. R. Evans, R. J. Pollard, A. V. Zayats, *Nano Lett.* **2008**, *8*, 281–296.
[24] S. Khatua, W. S. Chang, P. Swanglap, J. Olson, S. Link, *Nano Lett.* **2011**, *11*, 3797–3802.
[25] H. Zhang, Y. J. Li, I. A. Ivanov, Y. Q. Qu, Y. Huang, X. F. Duan, *Angew. Chem. Int. Ed.* **2010**, *49*, 2865–2868; *Angew. Chem.* **2010**, *122*, 2927–2930.
[26] Y. Liu, R. Cheng, L. Liao, H. L. Zhou, J. W. Bai, G. Liu, L. X. Liu, Y. Huang, X. F. Duan, *Nat. Commun.* **2011**, *2*, 579.
[27] Y. Q. Qu, R. Cheng, Q. Su, X. F. Duan, *J. Am. Chem. Soc.* **2011**, *133*, 16730–16733.
[28] H. T. Chen, W. J. Padilla, M. J. Cich, A. K. Azad, R. D. Averitt, A. J. Taylor, *Nat. Photonics* **2009**, *3*, 148–151.
[29] A. Kharkwal, M. Deepa, A. G. Joshi, A. K. Srivastava, *ChemPhysChem* **2011**, *12*, 1176–1188.
[30] M. Ozaki, J. Kato, S. Kawata, *Science* **2011**, *332*, 218–220.
[31] L. J. E. Anderson, K. M. Mayer, R. D. Fraleigh, Y. Yang, S. Lee, J. H. Hafner, *J. Phys. Chem. C* **2010**, *114*, 11127–11132.
[32] J. A. Osaheni, S. A. Jenekhe, H. Vanherzeele, J. S. Meth, Y. Sun, A. G. MacDiarmid, *J. Phys. Chem.* **1992**, *96*, 2830–2836.
[33] H. S. Nalwa, *Adv. Mater.* **1993**, *5*, 341–358.
[34] D. Li, J. X. Huang, R. B. Kaner, *Acc. Chem. Res.* **2009**, *42*, 135–145.
[35] N. R. Jana, L. Gearheart, C. J. Murphy, *Adv. Mater.* **2001**, *13*, 1389–1393.
[36] B. Nikoobakht, M. A. El-Sayed, *Chem. Mater.* **2003**, *15*, 1957–1962.
[37] S. X. Xing, L. H. Tan, M. X. Yang, M. Pan, Y. B. Lv, Q. H. Tang, Y. H. Yang, H. Y. Chen, *J. Mater. Chem.* **2009**, *19*, 3286–3291.
[38] L. Cristofolini, M. P. Fontana, P. Camorani, T. Berzina, A. Nabok, *Langmuir* **2010**, *26*, 5829–5835.
[39] M. J. Dicken, L. A. Sweatlock, D. Pacifici, H. J. Lezec, K. Bhattacharya, H. A. Atwater, *Nano Lett.* **2008**, *8*, 4048–4052.
[40] M. J. Polking, M. G. Han, A. Yourdkhani, V. Petkov, C. F. Kisielowski, V. V. Volkov, Y. M. Zhu, G. Caruntu, A. P. Alivisatos, R. Ramesh, *Nat. Mater.* **2012**, *11*, 700–709.
[41] K. S. Lee, M. A. El-Sayed, *J. Phys. Chem. B* **2005**, *109*, 20331–20338.
[42] H. J. Chen, X. S. Kou, Z. Yang, W. H. Ni, J. F. Wang, *Langmuir* **2008**, *24*, 5233–5237.
[43] S. A. Empedocles, M. G. Bawendi, *Science* **1997**, *278*, 2114–2117.
[44] K. Park, Z. Deutsch, J. J. Li, D. Oron, S. Weiss, *ACS Nano* **2012**, *6*, 10013–10023.
[45] Sub-wavelength refers to a particle with dimensions less than the wavelength of administered light.

Received: September 14, 2015
Revised: October 29, 2015
Published online: November 24, 2015

  